Modal Analysis of an Anisotropic Multilayer Slab Waveguide

Kiyoshi KISHIOKA*, Junji IWAO** and Katsu ROKUSHIMA*

(Received June 4, 1977)

This paper describes a method for analyzing the wave modes of a multilayer slab waveguide consisting of anisotropic dielectrics having arbitrary permittivity and permeability tensors. The propagation constants, the transmission matrix and the normal modes of the waves in the transverse direction are obtained as an eigenvalue problem of the coupling matrix derived from Maxwell's equations. The characteristic field equation is expressed in terms of matrix formulation which can be readily calculated with a computer. Furthermore, an exact expression for the coupling characteristics between TE and TM components of guided modes are given. Some numerical examples are also presented.

1. Introduction

Optical waveguides consisting of anisotropic materials have recently been of considerable interest in integrated optics because of the important role they play in applications such as mode convertors, modulators, isolators and circulators. The operation of devices containing anisotropic dielectrics depends[1)~3)] on the properties of the electromagnetic waves guided by the structure. These waves appear as characteristic solution of the boundary value problem of anisotropic multilayer slab waveguide.[4)] Then the problem of the wave modes in these guides have also been investigated for several specific structures as the basic concept for the applications.

The anisotropy of the materials constructing such waveguides are characterized by the permittivity and permeability tensors. When the values of the nondiagonal elements of these tensors are small and consequently the coupling between TE and TM components of the guided waves is weak, the wave-guiding properties have approximately been analyzed by using the variational method or the ray optics and the covenient expression have been presented.[5)] As the values of the nondiagonal elements become large the above approximation leads to erroneous results. In such a case of strong coupling, rigorous treatments based on the electromagnetic wave theory is necessary. However, the solutions of this problem have so far been limited in special cases with permittivity tensor having some zero elements.[6)]

The Authors have rigorously analyzed the wave modes of multilayer slab waveguide consisting of uniaxial anisotropic dielecrics by using a transverse equivalent circuit representation.[7)] In this paper, we extend the method to more general

* Department of Electlical Engineering, College of Engineering.
** Undergraduate Student, Department of Electrical Engineering, College of Engineering.

waveguides with anisotropic materials having arbitrary permittivity and permeability tensors.[8] Coupled equations representing the propagation of the fields in the transverse direction are derived and the propagation constants, the normal modes and the transmission matrix in this direction are obtained as an eigenvalue problem of the coupling matrix. Using them, the characteristic equation is expressed in terms of matrix formulation. Wave mode characteristics of the guide are then obtained by simple iterative calculation of matrices which are suited for computer analysis.

Furthermore, the coupling characteristics between TE and TM components of the guided waves are given exactly from the mode field distributions and the results are conveniently expressed by a quadratic form of guided mode amplitudes. Some numerical examples are also shown to discuss the reciprocity and nonreciprocity of the mode and coupling characteristics.

2. Matrix Representation of Propagation of Electromagnetic Waves in Anisotropic Material

Two-dimensional multilayer slab waveguide consisting of anisotropic dielectrics is shown in Fig. 1. The propagation direction of the electromagnetic fields and the normal direction to the interface are in the z and the x axes, respectively. In this coordinate, the permittivity tensor $\varepsilon_0\hat{\kappa}$ and the permeability tensor $\mu_0\hat{\mu}$ of the i-th layer are expressed as follows:

$$\hat{\kappa}=\begin{pmatrix} \kappa_{11} & \kappa_{21} & \kappa_{13} \\ \kappa_{21} & \kappa_{22} & \kappa_{23} \\ \kappa_{31} & \kappa_{32} & \kappa_{33} \end{pmatrix}, \qquad \hat{\mu}=\begin{pmatrix} \mu_{11} & \mu_{12} & \mu_{13} \\ \mu_{21} & \mu_{22} & \mu_{23} \\ \mu_{31} & \mu_{32} & \mu_{33} \end{pmatrix}, \tag{1}$$

where the subscript i is omitted for simplicity. In the each layer, the fields are

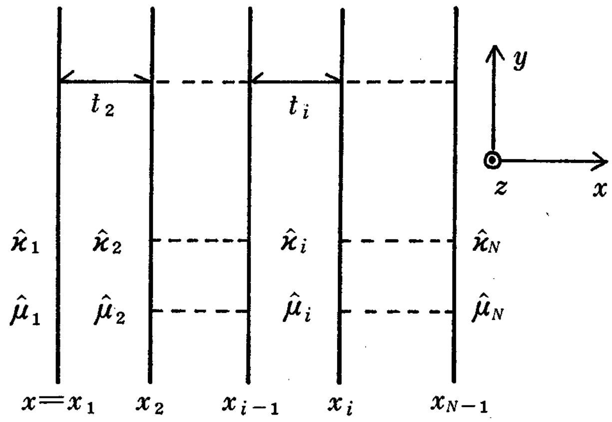

Fig. 1. Cross-sectional geometry of the multilayer slab waveguide

governed by Maxwell's equations:

$$\left.\begin{aligned} \nabla\times\boldsymbol{H}&=\varepsilon_0\hat{\kappa}\partial\boldsymbol{E}/\partial t\\ \nabla\times\boldsymbol{E}&=-\mu_0\hat{\mu}\partial\boldsymbol{H}/\partial t.\end{aligned}\right\}\tag{2}$$

Expressing the tangential and normal components of the fields to the interface as follows:

$$\boldsymbol{a}=[E_yH_zE_zH_y]^t,\qquad \boldsymbol{b}=[E_xH_x]^t\tag{3}$$

and assuming the wave mode of an $f(x)\exp[-j(\beta_z z-\omega t)]$ dependence for the fields, we can derive the following simultaneous differential equations from Eq. (2):

$$\partial\boldsymbol{a}/\partial x=\hat{C}\boldsymbol{a},\tag{4}$$

$$\boldsymbol{b}=\hat{D}\boldsymbol{a},\tag{5}$$

where

$$\hat{C}=\begin{pmatrix} \dfrac{\beta_z\mu_{31}}{\mu_{11}} & \dfrac{\omega\mu_0(\mu_{13}\mu_{31}-\mu_{11}\mu_{33})}{\mu_{11}} & 0 & \dfrac{\omega\mu_0(\mu_{12}\mu_{31}-\mu_{11}\mu_{32})}{\mu_{11}} \\[2ex] \dfrac{\kappa_{11}\beta_z^2+k_0^2\mu_{11}(\kappa_{12}\kappa_{21}-\kappa_{11}\kappa_{22})}{\omega\mu_0\mu_{11}\kappa_{11}} & \dfrac{\beta_z\mu_{13}}{\mu_{11}} & \dfrac{\omega\varepsilon_0(\kappa_{13}\kappa_{21}-\kappa_{11}\kappa_{23})}{\kappa_{11}} & \dfrac{\beta_z(\kappa_{11}\mu_{12}-\kappa_{21}\mu_{11})}{\kappa_{11}\mu_{11}} \\[2ex] \dfrac{\beta_z(\kappa_{12}\mu_{11}-\kappa_{11}\mu_{21})}{\kappa_{11}\mu_{11}} & \dfrac{\omega\mu_0(\mu_{11}\mu_{23}-\mu_{13}\mu_{21})}{\mu_{11}} & \dfrac{\beta_z\kappa_{13}}{\kappa_{11}} & \dfrac{k_0^2\kappa_{11}(\mu_{11}\mu_{22}-\mu_{12}\mu_{21})-\mu_{11}\beta_z^2}{\omega\varepsilon_0\kappa_{11}\mu_{11}} \\[2ex] \dfrac{\omega\varepsilon_0(\kappa_{11}\kappa_{32}-\kappa_{12}\kappa_{31})}{\kappa_{11}} & 0 & \dfrac{\omega\varepsilon_0(\kappa_{11}\kappa_{33}-\kappa_{13}\kappa_{31})}{\kappa_{11}} & \dfrac{\beta_z\kappa_{31}}{\mu_{11}} \end{pmatrix},\tag{6}$$

$$\hat{D}=\begin{pmatrix} -\kappa_{12}/\kappa_{11} & 0 & -\kappa_{13}/\kappa_{11} & \beta_z/\omega\varepsilon_0\kappa_{11} \\ -\beta_z/\omega\mu_0\mu_{11} & -\mu_{13}/\mu_{11} & 0 & -\mu_{12}/\mu_{11} \end{pmatrix}\tag{7}$$

and $\hat{C}$ is a coupling matrix whose 2×2 sub-matrices on the nondiagonal contribute to the coupling between TE and TM components.

The propagation constants β_{xi} in the x direction are obtained from the eigenvalue equation of $\hat{C}$:

$$\beta_x^4+\sum_{i=1}^{4}(-1)^i\Delta_i\beta_x^{4-i}=0\,,\tag{8}$$

where Δ_i is the sum of the i-dimensional principal minors of $\hat{C}$. For loss free materials, both $\hat{\kappa}$ and $\hat{\mu}$ are Hermitian, and Δ_i are all the real values. Therefore, if Eq. (8) has complex roots, their complex conjugate values are also the roots of this equation. In the following discussion, it is assumed that β_{xi} are non-degenerate. By right-eigenvectors $\boldsymbol{e}_i$ and left-eigenvectors $\boldsymbol{d}_i^+$ corresponding to β_{xi} $(i=1\sim4)$, the diagonalizer of $\hat{C}$ and its inverse matrix respectively are expressed in the useful form:

$$\hat{T}=[e_1/\sqrt{s_{11}}\;\; e_2/\sqrt{s_{22}}\;\; e_3/\sqrt{s_{33}}\;\; e_4/\sqrt{s_{44}}] \tag{9}$$

and

$$\hat{T}^{-1}=[d_1^*/\sqrt{s_{11}}\;\; d_2^*/\sqrt{s_{22}}\;\; d_3^*/\sqrt{s_{33}}\;\; d_4^*/\sqrt{s_{44}}]^t, \tag{10}$$

where $S_{ii}=d_i^+\cdot e_i$ and $*$, t and $+$ denote the complex conjugate, the transpose and the complex-conjugate transpose, respectively.

The solution of Eq. (4) is

$$a=\exp[j\hat{C}(x-x_0)]\,a_{x0}, \tag{11}$$

where a_{x0} represents the fields at a arbitrary point x_0. In this equation, $\exp[j\hat{C}(x-x_0)]$ represents the transmission matrix of a in the x direction. Expanding it in the form of power series and using the following relation:

$$\hat{T}^{-1}\hat{C}\hat{T}=\mathrm{diag}[\beta_{x1}\;\beta_{x2}\;\beta_{x3}\;\beta_{x4}], \tag{12}$$

we can transform the transmission matrix into

$$\hat{A}=\hat{T}\ \mathrm{diag}[\exp(j\beta_{x1}l)\ \exp(j\beta_{x2}l)\ \exp(j\beta_{x3}l)\ \exp(j\beta_{x4}l)]\hat{T}^{-1}, \tag{13}$$

where $l=x-x_0$.

The tangential components a can be decomposed into the normal modes e_i ($i=1\sim4$), which propagate independently in the x direction with the propagation constants β_{xi}, and the amplitude vector g of normal modes is introduced as follows:

$$a=\sum_{i=1}^{4} g_i e_i/\sqrt{s_{ii}}=\hat{T}g, \tag{14}$$

where g_i is the i-th component of g and it can be defined by multiplying $\hat{T}^{-1}$ by Eq. (14). That is

$$g_i=(d_i^+\cdot a)/\sqrt{s_{ii}}\quad (i=1\sim4). \tag{15}$$

The substitution of Eqs. (12) and (13) into Eq. (11) yields the following relation for g:

$$g=\mathrm{diag}[\exp(j\beta_{x1}l)\ \exp(j\beta_{x2}l)\ \exp(j\beta_{x3}l)\ \exp(j\beta_{x4}l)]\ g_{x0}. \tag{16}$$

This equation characterizes the propagation of g. As g is given at x_0, the field distributions at the arbitrary point in the layer can be obtained by Eqs. (14), (13) and (5).

Generally, both β_{xi} and e_i can be obtained by solving numerically the eigenvalue problem of $\hat{C}$. However, in the following special cases, β_{xi} are analytically given as the solution of Eq. (8).

(i) For the longitudinal type

$$\beta_{xi}^2=[\{k_0^2(\kappa_{11}\kappa_{33}-\kappa_{11}\kappa_{22}+\kappa_{12}\kappa_{21})-\beta_z^2(\kappa_{11}+\kappa_{22})\} \pm\sqrt{\{k_0^2(\kappa_{11}\kappa_{33}-\kappa_{11}\kappa_{22}+\kappa_{12}\kappa_{21})-\beta_z^2(\kappa_{11}+\kappa_{22})\}^2-4\kappa_{11}\kappa_{33}\{(k_{11}^2-\beta_z^2)(k_{22}^2-\beta_z^2)-k_{12}^2k_{21}^2\}}\,]/2\kappa_{11} \tag{17}$$

(ii) For the polar type

$$\beta_{xi}^2=[\{k_{11}^2(\kappa_{22}+\kappa_{33})-\beta_z^2(\kappa_{11}+\kappa_{33})\}$$
$$\pm\sqrt{\{k_{11}^2(\kappa_{22}+\kappa_{33})-\beta_z^2(\kappa_{11}+\kappa_{33})\}^2-4\kappa_{11}(k_{11}^2-\beta_z^2)\{(k_{22}^2-\beta_z^2)\kappa_{33}-k_0^2\kappa_{23}\kappa_{32}\}}]/2\kappa_{11} \quad (18)$$

(iii) For the equatorial type

In this case, Eq. (6) becomes the following form:

$$\hat{C}=\begin{pmatrix}\hat{C}_e & 0\\ 0 & \hat{C}_m\end{pmatrix}. \quad (19)$$

Consequently, TE and TM components are separable and β_{xi} corresponding to $\hat{C}_e$ and $\hat{C}_m$ are also given separately as

$$\beta_{x2}^{\,1}=\pm\sqrt{k_{22}^2-\beta_z^2} \text{ (TE)} \quad (20)$$

and

$$\beta_{x4}^{\,3}=[\beta_z(\kappa_{13}+\kappa_{31})\pm\sqrt{\beta_z^2(\kappa_{13}+\kappa_{31})^2-4(k_{11}^2-\beta_z^2)(\kappa_{11}\kappa_{33}-\kappa_{13}\kappa_{31})}]/2\kappa_{11} \text{ (TM)}. \quad (21)$$

In isotropic media, β_{xi} are obtained by putting $\kappa_{ij}=\delta_{ij}\kappa$ in Eqs. (20) and (21):

$$\beta_{x24}^{\,13}=\pm\sqrt{k_0^2\kappa-\beta_z^2}\,, \quad (22)$$

where $k_{ij}^2=k_0^2\kappa_{ij}$ and $\mu_{ij}=\delta_{ij}$.

3. Derivation of the Characteristic Equation

The tangential components between the two interfaces at $x=x_{i-1}$ and x_i of the i-th layer are related to each other by the transmission matrix $\hat{A}_i$, which is given by putting $l=t_i$ in Eq. (13), and must be continuous across the interfaces. Therefore, $\boldsymbol{a}_{x1}$ at $x=x_1$ and $\boldsymbol{a}_{xN-1}$ at $x=x_{N-1}$ are related by

$$\boldsymbol{a}_{xN-1}=(\prod_{i=2}^{N-1}\hat{A}_i)\boldsymbol{a}_{x1}\equiv\hat{\boldsymbol{F}}\boldsymbol{a}_{x1}\,. \quad (23)$$

The substitution of Eq. (14) into Eq. (23) leads to the following similar relation for $\boldsymbol{g}$:

$$g_{xN-1}=\hat{T}_N^{-1}\hat{F}\hat{T}_1 g_{x1}\,, \quad (24)$$

where $\hat{T}_i$ is $\hat{T}$ of the i-th layer. In the surrounding two layers, fields should be vanishing at $x=\pm\infty$ for guided modes. Therefore, the two normal modes, which have two propagation constants $\beta_{x\,l}^{\,k}$ with the condition Im $(\beta_x)<0$ in the first layer and have $\beta_{x\,n}^{\,m}$ with the condition Im $(\beta_x)>0$ in the last layer, are permitted to exist. Considering the above condition, we put

$$g_{ix1}=0\ (i\neq k,\, l), \quad g_{ixN-1}=0\ (i\neq m,\, n). \quad (25)$$

By using the suitable matrix $\hat{W}$, which is formed by exchanging the elements of $\hat{T}_N^{-1}\hat{F}\hat{T}_1$, Eq. (24) can be transformed as follows:

$$[0\ 0\ g_m g_n]_{xN-1}^t=\hat{W}[g_k g_l\ 0\ 0]_{x1}^t\,. \quad (26)$$

These are four homogeneous simultaneous linear equations for g_k, g_l, g_m and g_n. Therefore, characteristic equation for guided modes is given by

$$\det\left(\begin{bmatrix} w_{11} & w_{12} \\ w_{21} & w_{22} \end{bmatrix}\right)=0\,, \tag{27}$$

where w_{ij} represents the element in the i-th row, the j-th column of $\hat{W}$. From Eq. (26), the ratio of g_l to g_k of the guided mode at $x=x_1$ is given by

$$(g_l/g_k)_{x1}=-w_{11}/w_{12}=-w_{21}/w_{22}\,. \tag{28}$$

As the ratio of the normal mode amplitudes is decided, the relative values of the field components can be calculated by Eq. (14) and $\hat{A}$.

The characteristics of the guided modes propagating in the negative z direction can be obtained similarly by analyzing for $\beta z<0$.

4. Numerical Examples of the Modal Analysis

(1) We consider the waveguide with the permittivity tensor having all non-zero elements. The permittivity tensor of each layer is given as ε_3^1: $[\varepsilon_0]$, $\hat{\varepsilon}_2$: $[\hat{\kappa}_p$: $(\kappa_{11}=4.0$, $\kappa_{22}=3.0$, $\kappa_{33}=2.0$, $\kappa_{23}=\kappa_{32}{}^*=j)$, $\varphi=\theta=\pi/4]$, where $\hat{\kappa}_p$ is the permittivity tensor in

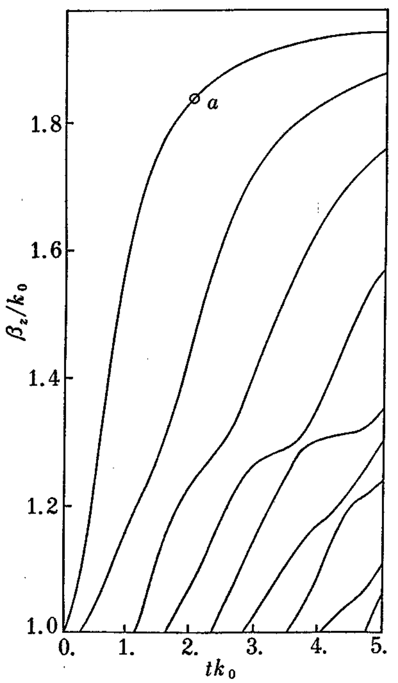

Fig. 2. Normalized propagation constants $\beta_z/k_0 - tk_0$ characteristics of the slab waveguide with the permittivity tensor having all non-zero elements

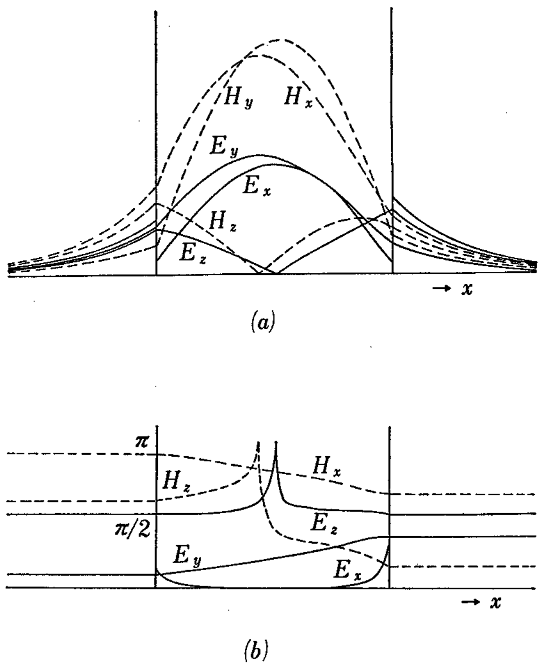

Fig. 3. Field distributions at the point a in Fig. 2.
(a) Absolute values of the fields
(b) Difference of phase between H_y and the other components

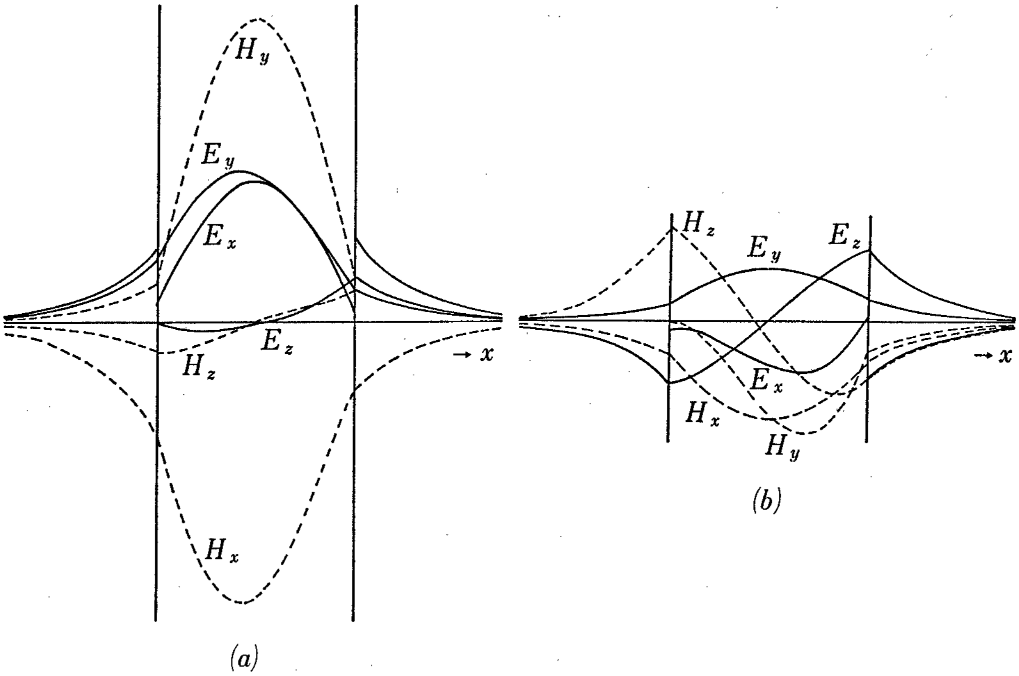

Fig. 4. Instantaneous values of the fields
(a) Fields at $z=0$
(b) Fields at $z=\lambda_g/4$

the coordinate $\xi-\eta-\zeta$, φ is the angle made by y and η axes and θ is the angle made by x and ξ axes. The thickness of the waveguide is $2t$ and the permeability is μ_0 in each layer. The propagation constants β_z obtained by solving numerically Eq. (27) are shown in Fig. 2. The absolute values of the field components of the guided mode and the difference of phase between H_y and the other field components are shown in Figs. 3-(a) and (b).

Since the field components have complex values in the transverse plane, patterns of the field distributions vary with time, which are shown in Fig. 4.

(2) For waveguides with $\hat{\kappa}$ varying continuously in the x direction, the characteristics can be approximately obtained by dividing the waveguide into multilayer slabs. For this example, we consider the waveguide whose permittivity tensors are; ε_3^1: $[\varepsilon_0]$, $\hat{\varepsilon}_2$: $[\kappa_{ii}(x)=\left\{\begin{smallmatrix}4.\\3.\\2.\end{smallmatrix}\right\}\exp(-0.14x),\ \kappa_{12}=\kappa_{21}^*=j]$ and whose thickness is $2t$. When the slab is devided into eight layers, the propagation constants β_z of the guided modes and the field distributions of a specific mode are shown in Figs. 5 and 6, respectively. For comparison, the characteristics of the waveguide having the constant permittivity tensor, whose elements are the values at $x=0$, are also shown by dotted curves in Fig. 5.

The wave-guiding properties of the isolated waveguides dealt with in (1) and (2) are reciprocal with the direction of the wave propagation. However, in some

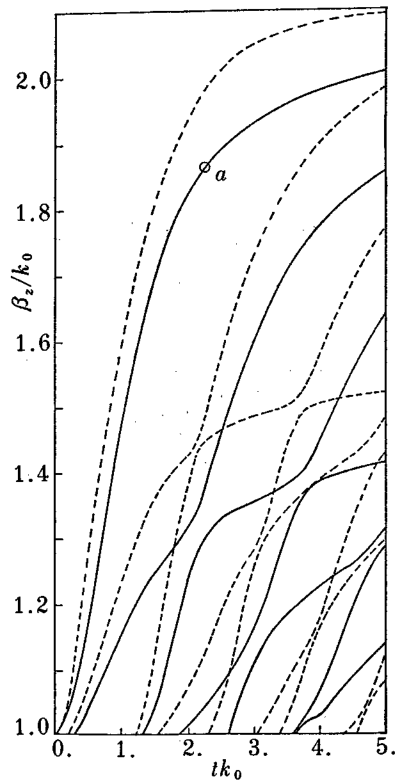

Fig. 5. Normalized propagation constants β_z/k_0-tk_0 characteristics of the slab waveguide in which the permittivity tensor varies exponentially in the x direction. (real curves)

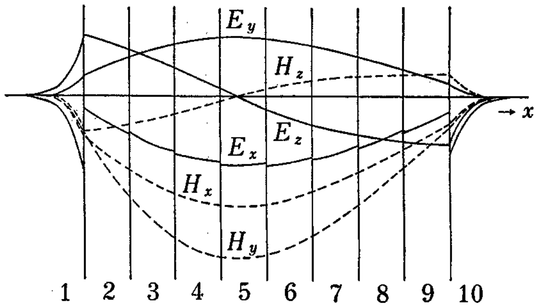

Fig. 6. Field distributions at the point a in Fig. 5

kinds of waveguides consisting of both the gyrotropic and the anisotropic media, for example, GL-AP, GE-AL, or GE-AP type, these properties are shown to be nonreciprocal, therefore, these guides will have many applications to nonreciprocal optical-devices.

5. TE-TM Mode Conversion

In this section we consider the coupling between TE and TM components of the fields composed of several guided modes.

By a linear combination of the guided modes, we express the total fields as follows:

$$\left.\begin{aligned} \boldsymbol{E}(x, z) &= \sum_i h_i \boldsymbol{E}_i(x) \exp(-j\beta_{zi}z) \\ \boldsymbol{H}(x, z) &= \sum_i h_i \boldsymbol{H}_i(x) \exp(-j\beta_{zi}z), \end{aligned}\right\} \tag{29}$$

where $\boldsymbol{E}_i(x) \exp(-j\beta_{zi}z)$ and $\boldsymbol{H}_i(x) \exp(-j\beta_{zi}z)$ represent the guided mode fields and

h_i is the mode amplitude. The total available power propagating in the z direction is

$$P_t = P_{te}(z) + P_{tm}(z) = Re\{\textstyle\int_{-\infty}^{\infty} (\boldsymbol{E} \times \boldsymbol{H}^*) \cdot \boldsymbol{i}_z \, \mathrm{d}x\}, \tag{30}$$

where $P_{te}(z) = -Re\{\int_{-\infty}^{\infty} H_x{}^* E_y \mathrm{d}x\}$, $P_{tm}(z) = Re\{\int_{-\infty}^{\infty} H_y{}^* E_x dx\}$ and $\boldsymbol{i}_z$ represents the unit vector along the z axis. By using the orthogonal relation*:

$$\textstyle\int_{-\infty}^{\infty} (\boldsymbol{E}_i \times \boldsymbol{H}_j{}^* + \boldsymbol{E}_j{}^* \times \boldsymbol{H}_i) \cdot \boldsymbol{i}_z \, \mathrm{d}x = 0 \, (i \neq j), \tag{31}$$

Eq. (30) becomes

$$P_t = \sum_i [h_i{}^* h_i Re\{\textstyle\int_{-\infty}^{\infty} (\boldsymbol{E}_i \times \boldsymbol{H}_i{}^*) \cdot \boldsymbol{i}_z \, \mathrm{d}x]. \tag{32}$$

We normalize the available power of the each mode into unit and furthermore, normalize the total available power as follows:

$$P_t = \boldsymbol{h}^+ \cdot \boldsymbol{h} = 1, \tag{33}$$

where $\boldsymbol{h}$ is the normalized mode amplitude vector with element h_i. The available power of TE components can be expressed in terms of the quadratic form of $\boldsymbol{h}$, that is

$$\begin{aligned} P_{te}(z) &= \{\boldsymbol{h}^+ \hat{U} (\hat{P}^+ + \hat{P}) \hat{U}^* \boldsymbol{h}\}/2 \\ &\equiv \boldsymbol{h}^+ \hat{Q} \boldsymbol{h}, \end{aligned} \tag{34}$$

where $\hat{P}$ is the matrix whose elements are defined by $p_{ij} = -\int_{-\infty}^{\infty} H_{xi}{}^* E_{yj} \mathrm{d}x$ and $\hat{U} = \mathrm{diag}[\exp(j\beta_{zi} z)]$.

When $\boldsymbol{h}$ is given at $z=0$, the variation of $P_{te}(z)$, in the other words the power transfer from TM components, can be expressed as follows:

$$\begin{aligned} P_c(z) &= \boldsymbol{h}^+ (\hat{U} \hat{Q} \hat{U}^* - \hat{Q}) \boldsymbol{h} \\ &= 2 \sum_{i,j(i<j)} |q_{ij}| \cdot [-2\cos(\phi_i - \phi_j - \psi_{ij}) \sin^2\left(\frac{\beta_{zi} - \beta_{zj}}{2} z\right) \\ &\qquad + \sin(\beta_{zi} - \beta_{zj}) z \cdot \sin(\phi_i - \phi_j - \psi_{ij})] \cdot |h_i h_j|, \end{aligned} \tag{36}$$

where $h_i = |h_i| \exp(j\phi_i)$ and $q_{ij} = |q_{ij}| \exp(j\psi_{ij})$ which is the element in the i-th row, the j-th column of $\hat{Q}$. And note that $\hat{Q}$ is Hermitian.

Next we minimize P_{te} in order to obtain the maximum power transfer. When $\boldsymbol{h}$ is the normalized eigenvector corresponding to the minimum eigenvalue of $\hat{Q}$, P_{te} has the minimum value under the condition of Eq. (33). After minimizing P_{te}, we can define the optimum coupling coefficient C_0 as the maximum value of P_C and the coupling length L as the distance from $z=0$, at which P_C becomes the maximum value. If p_{12} and p_{21} are real values in the two-mode coupling, Eq. (36) can be transformed into the simple form:

$$P_C(z) = 4|q_{12}| \cdot |h_1 h_2| \sin^2\left(\frac{\beta_{z1} - \beta_{z2}}{2} z\right). \tag{37}$$

---

* This orthogonal relation can be also derived in the waveguide with Hermitian $\hat{\varepsilon}$ and $\hat{\mu}$ as well as with real $\hat{\varepsilon}$.[9]

C_0 and L in this case are given as

$$C_0=4|q_{12}|\cdot|h_1h_2| \tag{38}$$

and

$$L=\pi/|\beta_{z1}-\beta_{z2}|\,. \tag{37}$$

We can similarly define the optimum coupling coefficient and the coupling length by P_{tm}, but the minimum value of P_{tm} when P_{te} is minimized is generally larger than that when P_{tm} is minimized. The coupling characteristics obtained in the two cases, are therefore not identical.

6. Numerical Examples of the Mode Conversion

(1) The variation of C_0 versus tk_0 in the two-mode coupling is shown in Fig. 7 with the parameter κ_{12}. The waveguide is surrounded by free space and the permittivity tensor is given in Fig. 7. For all κ_{12}, the power of TE components transfers perfectly into that of TM at the point $tk_0\simeq1.393$. This point is the degenerate point of the TE and TM dominant modes when $\kappa_{12}=0.0$.

(2) As an example of the multimode coupling, we consider again the waveguide dealt with in the section 4–(1). The field distributions, composed of all the four modes at $tk_0=2.0$ in the condition of minimizing P_{te} at $z=0$, are shown Fig. 8-(a) and power transfer in the z direction is shown Fig. 8-(b).

(3) As a nonreciprocal mode conversion, we consider the two-layer waveguide consisting of the anisotropic materials having GL type of $\hat{\kappa}$ and AP type of $\hat{\kappa}$. C_0 and L of the forward and backward wave modes are shown in Fig. 9. We assume that the permittivity tensors are; ε_4^1: $[\varepsilon_0]$, $\hat{\varepsilon}_2$: $[\kappa_{11}=4.0$, $\kappa_{22}=3.0$, $\kappa_{33}=2.0$, $\kappa_{12}=\kappa_{21}{}^*=$

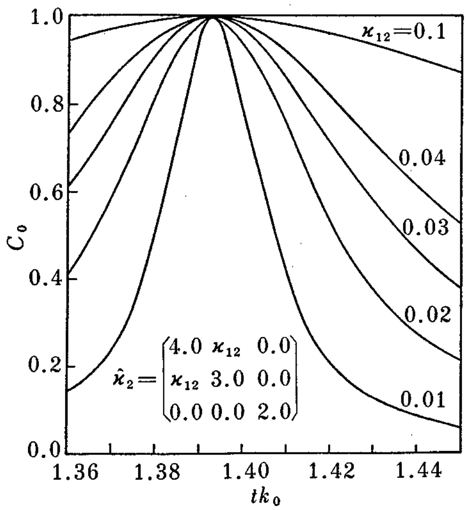

Fig. 7. Optimum coupling coefficient-tk_0 characteristics of the waveguide with the AL type of permittivity tensor

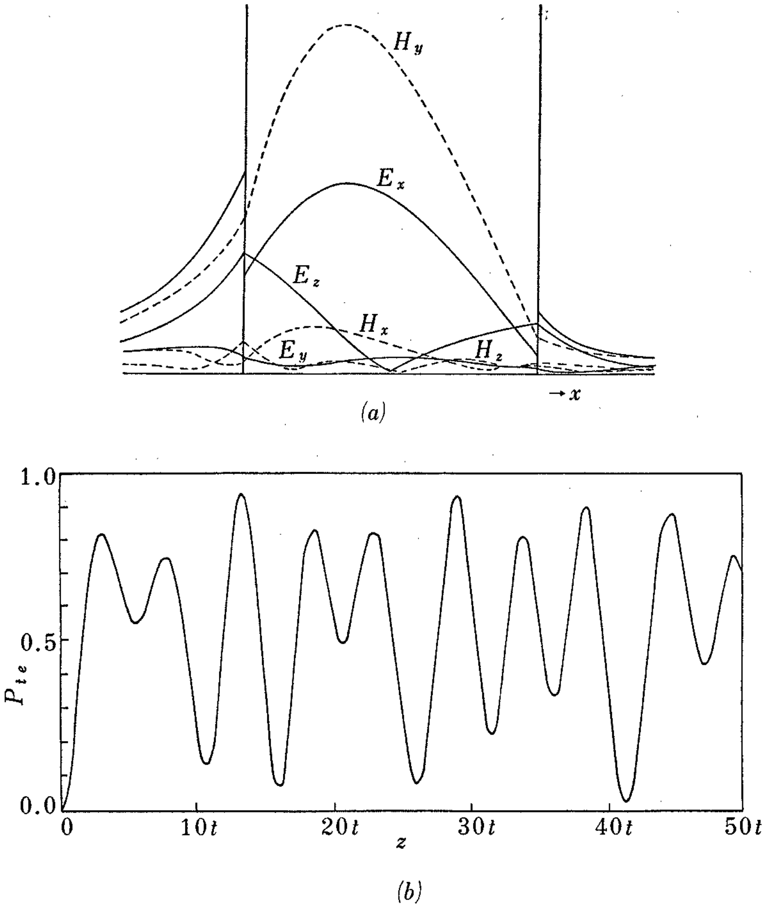

Fig. 8. Characteristics of multimode coupling
(a) Field distributions composed in the condition of minimizing P_{te} at $z=0$
(b) Power transfer in the z direction

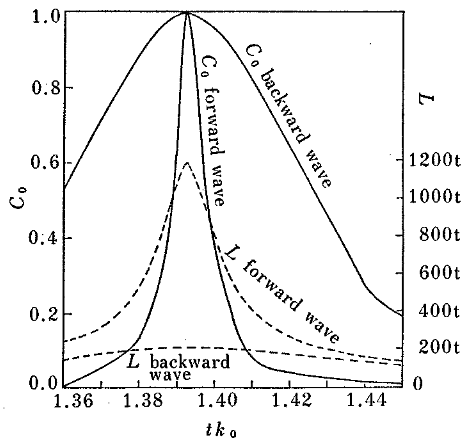

Fig. 9. Optimum coefficient and coupling length-tk_0 characteristics in the nonreciprocal waveguide

$0.03j$], $\hat{\varepsilon}_3$: [$\kappa_{11}=4.0$, $\kappa_{22}=3.0$, $\kappa_{33}=2.0$, $\kappa_{23}=\kappa_{32}=0.03$] and the thickness of the slabs are; $t_2=t$, $t_3=t$.

7. Conclusion

We have analyzed the wave modes of the waveguide consisting of the materials having arbitrary permittivity and permeability tensors in terms of matrix formulation. Since the characteristic field equation have been derived by the eigenvalue problem and the iterative matrix calculation, this equation have been solved conveniently by a computer. In the case of involving lossy media, though β_z become complex values, we can similarly analyze by devising the solution of the characteristic equation.

The optimum coupling coefficient and the coupling length in the TE and TM mode conversion of the multimode waveguide have been given exactly from the mode field distributions, and the nonreciprocity of them in the waveguide with both the gyrotropic and the anisotropic type of media have been shown in the numerical example.

We expect that this method will be similarly applied to the analysis of the radiation modes in such an anisotropic slab waveguide.

Acknowledgement

The Authors would like to thank Mr. S. Mori and Mr. M. Kominami for their helpful discussions and suggestions.

References

1) S. Wang, M. Shar and J. D. Crow, J. Appl. Phys., **43**, 1861 (1974).
2) D. Marcuse, Trans. IEEE, **QE-11**, 759 (1975).
3) J. Warner, Trans. IEEE, **MTT-23**, 70 (1975).
4) M. O. Vassell, J. Opt. Soc. Amer., **64**, 166 (1974).
5) S. Yamamoto and T. Makimoto, Trans. IECE Japan, **56-C**, 187 (1973).
6) Y. Satomura, M. Matsuhara and N. Kumagai, Trans. IEEE, **MTT-22**, 86 (1974).
7) K. Rokushima, K. Kishioka, S. Mori and M. Kominami, Trans. IECE Japan, **59-C**, 363, (1976).
8) K. Kishioka and K. Rokushima, Lecture 337 in Annual Meeting of IECE Japan, (Nov.-1976).
9) D. Marcuse, Bell Syst. Tech. J., **54**, 985 (1975).